

## Interfacial reaction depending on the stack structure of Al<sub>2</sub>O<sub>3</sub> and HfO<sub>2</sub> during film growth and postannealing

M.-H. Cho, K. B. Chung, H. S. Chang, D. W. Moon, S. A. Park, Y. K. Kim, K. Jeong, C. N. Whang, D. W. Lee, D.-H. Ko, S. J. Doh, J. H. Lee, and N. I. Lee

Citation: *Applied Physics Letters* **85**, 4115 (2004); doi: 10.1063/1.1807968

View online: <http://dx.doi.org/10.1063/1.1807968>

View Table of Contents: <http://scitation.aip.org/content/aip/journal/apl/85/18?ver=pdfcov>

Published by the [AIP Publishing](#)

---

### Articles you may be interested in

[Thin HfO<sub>2</sub> films grown on Si \( 100 \) by atomic oxygen assisted molecular beam epitaxy](#)

*Appl. Phys. Lett.* **85**, 85 (2004); 10.1063/1.1767604

[Film properties of ALD HfO<sub>2</sub> and La<sub>2</sub>O<sub>3</sub> gate dielectrics grown on Si with various pre-deposition treatments](#)

*J. Vac. Sci. Technol. B* **22**, 2121 (2004); 10.1116/1.1773840

[Effects of plasma nitridation of Al<sub>2</sub>O<sub>3</sub> interlayer on thermal stability, fixed charge density, and interfacial trap states of HfO<sub>2</sub> gate dielectric films grown by atomic layer deposition](#)

*J. Appl. Phys.* **94**, 1898 (2003); 10.1063/1.1590418

[Interfacial properties of ZrO<sub>2</sub> on silicon](#)

*J. Appl. Phys.* **93**, 5945 (2003); 10.1063/1.1563844

[Interfacial silicon oxide formation during oxygen annealing of Ta<sub>2</sub>O<sub>5</sub> thin films on Si: Oxygen isotope labeling](#)

*J. Vac. Sci. Technol. A* **18**, 2522 (2000); 10.1116/1.1286717

---

An advertisement for Keysight B2980A Series Picoammeters/Electrometers. The ad features a red and white color scheme. On the left, text reads 'Confidently measure down to 0.01 fA and up to 10 PΩ' and 'Keysight B2980A Series Picoammeters/Electrometers'. Below this is a red button with the text 'View video demo'. On the right, there is an image of the Keysight B2980A device, which is a small, rectangular electronic instrument with a screen and various ports. To the right of the device is the Keysight Technologies logo, which consists of a stylized red 'W' shape followed by the text 'KEYSIGHT TECHNOLOGIES'.

## Interfacial reaction depending on the stack structure of $\text{Al}_2\text{O}_3$ and $\text{HfO}_2$ during film growth and postannealing

M.-H. Cho,<sup>a)</sup> K. B. Chung, H. S. Chang, and D. W. Moon

*Nano Surface Group, Korea Research Institute of Standards and Science, DaeJeon 305-600, Korea*

S. A. Park, Y. K. Kim, K. Jeong, and C. N. Whang

*IPAP, Yonsei University, Seoul, 120-749, Korea*

D. W. Lee and D.-H. Ko

*Department of Ceramic Engineering, Yonsei University, Seoul 120-749, Korea*

S. J. Doh, J. H. Lee, and N. I. Lee

*System LSI Division, Samsung Electronics Co. Yongin-Si, Kyunggi-Do, 449-711, Korea*

(Received 9 March 2004; accepted 30 August 2004)

Interfacial reactions as a function of the stack structure of  $\text{Al}_2\text{O}_3$  and  $\text{HfO}_2$  grown on Si by atomic-layer deposition were examined by various physical and electrical measurements. In the case of an  $\text{Al}_2\text{O}_3$  film with a buffer layer of  $\text{HfO}_2$ , reactions between the  $\text{Al}_2\text{O}_3$  and Si layers were suppressed, while a  $\text{HfO}_2$  film with an  $\text{Al}_2\text{O}_3$  buffer layer on the Si readily interacted with Si, forming a Hf–Al–Si–O compound. The thickness of the interfacial layer increased dramatically after an annealing treatment in which a buffer layer of  $\text{Al}_2\text{O}_3$  was used, while no change in thickness was observed in the film in which a  $\text{HfO}_2$  buffer layer was used. Moreover, the stoichiometric change caused by a different reaction process altered the chemical state of the films, which affected charge trapping and the interfacial trap density. © 2004 American Institute of Physics. [DOI: 10.1063/1.1807968]

High-permittivity dielectrics have been widely investigated as alternative gate insulating layers in advanced MOS devices because high dielectric oxides permit the use of thicker films, compared to other oxides, such as  $\text{SiO}_2$ , which have a lower dielectric constant. The possible use of  $\text{HfO}_2$  based high dielectrics, in particular, have attracted considerable attention as a possible replacement for  $\text{SiO}_2$  in gate oxides of ULSI because of their thermal stability and high dielectricity.<sup>1,2</sup>  $\text{HfO}_2$  has a relatively high dielectric constant of 25–30, a low leakage current, and is highly reliable although the structural transition from amorphous to crystalline phase occurs at a low temperature and the material has a relatively small band gap (~5.5 eV).<sup>3</sup>

A number of reports have focused on the use of composites of two dielectric oxides or multilayers of dielectrics for the purpose of a achieving comparable dielectrics and to enhance thermal stability.<sup>4,5</sup> Mixed Al–Hf oxides have attracted particular attention because the transition temperature from amorphous to polycrystalline is increased, compared to pure  $\text{HfO}_2$  and  $\text{Al}_2\text{O}_3$ .<sup>6</sup> Johnson *et al.* reported that the flatband voltage shift of the Hf–Aluminate alloy is caused by electron trapping.<sup>7</sup> However, interfacial reactions between the high- $k$  oxide and the Si substrate were not considered, although the interfacial reaction at the contact of the dielectric with Si can affect intermixing, resulting in a significant change in thermal stability and flatband voltage shift.

In this study, we focused on the characteristics of bilayer  $\text{HfO}_2$ – $\text{Al}_2\text{O}_3$  films grown on Si using an atomic layer deposition (ALD) system. In particular, physical and electrical characteristics as a function of stack structure, whether Si is in contact with  $\text{HfO}_2$  or  $\text{Al}_2\text{O}_3$ , were investigated. The findings show that intermixing between  $\text{HfO}_2$  and  $\text{Al}_2\text{O}_3$  was significantly affected by the stack structure, resulting in a

different film stoichiometry as a result of interactions between the films and the Si substrate. The change in film thickness after annealing was also dependent on the stack structure, resulting in a drastic increase in total film thickness when a buffer layer of  $\text{Al}_2\text{O}_3$  was used, while it was suppressed in the case of an  $\text{Al}_2\text{O}_3$  film in which the buffer layer was  $\text{HfO}_2$ . As a result, we conclude that interfacial reactions and intermixing are suppressed in a film in which a buffer layer of  $\text{HfO}_2$  is used, compared to a film with a buffer layer of  $\text{Al}_2\text{O}_3$ .

The  $p$ -type Si substrate with 2–5  $\Omega$  cm was cleaned using the RCA method and then preprocessed to include a ~1.0 nm  $\text{SiO}_2$  layer to stabilize and reduce the interfacial state. The metal oxides were grown by means of an ALD system, which has a vertical warm wall reactor with a showerhead and a heated susceptor.  $\text{Al}_2\text{O}_3$  and  $\text{HfO}_2$  films were each grown at temperatures below 300 °C using  $\text{Al}(\text{CH}_3)_3$  and  $\text{HfCl}_4$  as a precursors.  $\text{H}_2\text{O}$  vapor served as the oxygen source and  $\text{N}_2$  was supplied as the purge and carrier gas. Bilayer structures with  $\text{HfO}_2(15 \text{ \AA})/\text{Al}_2\text{O}_3(30 \text{ \AA})/\text{Si}$  and  $\text{Al}_2\text{O}_3(30 \text{ \AA})/\text{HfO}_2(15 \text{ \AA})/\text{Si}$  were fabricated. In order to use the high thermal stability of  $\text{Al}_2\text{O}_3$  and compensate the negative trap charge in  $\text{Al}_2\text{O}_3$  with  $\text{HfO}_2$ , the  $\text{Al}_2\text{O}_3$  layer was thicker than the  $\text{HfO}_2$ . The films were annealed using a rapid thermal process in an ambient of  $\text{N}_2$  from 750 to 900 °C for 5 min.

The chemical state and stoichiometry of the films were investigated using x-ray photoelectron spectroscopy and medium energy ion scattering (MEIS) measurements. A MEIS analysis was accomplished with a 100 keV proton beam in a double alignment so as to reduce contributions from the crystalline Si substrate, allowing the deconvolution of the spectra into contributions from the  $\text{Al}_2\text{O}_3$  layer and Si signals. Pt dots with a 0.01 cm radius for a MOS diode were evaporated onto the oxide surface as electrodes.  $C$ – $V$  measurements

<sup>a)</sup>Electronic mail: mhcho@kriss.re.kr

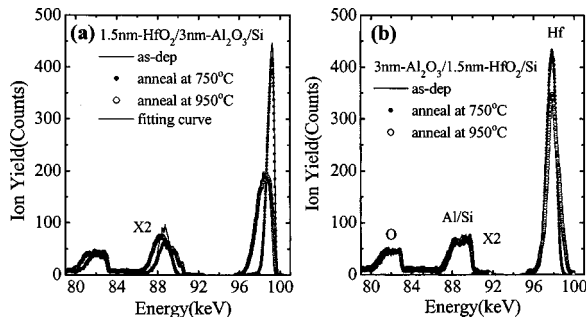


FIG. 1. MEIS spectra of (a) an HfO<sub>2</sub> film (15 Å) with a buffer layer of Al<sub>2</sub>O<sub>3</sub> (30 Å) on an oxidized Si and (b) Al<sub>2</sub>O<sub>3</sub> (30 Å) film with a buffer layer of HfO<sub>2</sub> film (15 Å) on an oxidized Si substrate. MEIS spectra of annealed films at 750 and 900 °C for 5 min in a N<sub>2</sub> ambient are also shown in (a) and (b).

were performed in a probe station using an HP 4284A instrument.

Changes in layer thickness and stoichiometry were investigated by MEIS measurements, as shown in Fig. 1. The calculated thickness of the as-grown Al<sub>2</sub>O<sub>3</sub> and HfO<sub>2</sub> films from MEIS spectra is about 32 and 14 Å, respectively when HfO<sub>2</sub> is used as a buffer layer. A very thin ~12 Å SiO<sub>2</sub> layer, which was formed before film growth to limit interfacial oxidation and to improve interfacial quality, was observed in the film in which Al<sub>2</sub>O<sub>3</sub> was used as a buffer layer, indicating that no interfacial reactions occurred between Al<sub>2</sub>O<sub>3</sub>/Si.<sup>8</sup> The interface between HfO<sub>2</sub>/Al<sub>2</sub>O<sub>3</sub> is quite sharp and no interdiffusion was observed. The most important finding is that intermixing between HfO<sub>2</sub> and Al<sub>2</sub>O<sub>3</sub> is dependent on which buffer layer is in contact with the Si. The depth profile of an as-grown film in the stack structure of Al<sub>2</sub>O<sub>3</sub>/HfO<sub>2</sub>/Si is almost the same as that for a film annealed at 750 °C, while that of HfO<sub>2</sub>/Al<sub>2</sub>O<sub>3</sub>/Si was altered somewhat. Slight changes in the peak heights of Al/Si and Hf indicate that interdiffusion between HfO<sub>2</sub> and Al<sub>2</sub>O<sub>3</sub> starts at an annealing temperature of 750 °C. The difference in the depth profile of the annealed samples at 900 °C indicates that the HfO<sub>2</sub> and Al<sub>2</sub>O<sub>3</sub> layers were completely intermixed in the stack structure of HfO<sub>2</sub>/Al<sub>2</sub>O<sub>3</sub>/Si, while two layers were intermixed slightly in the stack structure of Al<sub>2</sub>O<sub>3</sub>/HfO<sub>2</sub>/Si. Another noteworthy change is that small amounts of Si on the film surface after a 900 °C annealing treatment is observed when Al<sub>2</sub>O<sub>3</sub> is used as a buffer layer. Thus, the diffusion of Si to the upper film occurs, although silicate formation in an as-grown film is effectively suppressed compared to the as-grown Al<sub>2</sub>O<sub>3</sub>/HfO<sub>2</sub>/Si stack structure. The Si on film surface indicates that Si diffusion is closely related to the drastic interdiffusion of HfO<sub>2</sub> and Al<sub>2</sub>O<sub>3</sub>, i.e., the diffusion of Si from the bottom layer enhances interdiffusion. Moreover, a difference in the peak width of O between two stack structures shows that the increase of the oxide layer thickness by more than 10 Å occurs only in the HfO<sub>2</sub>/Al<sub>2</sub>O<sub>3</sub>/Si stack structure annealed at 900 °C, which is caused by the oxidation of Si layer at the film surface diffused from Si substrate.

Changes in the stack structure were also investigated using HRTEM, as shown in Fig. 2. The TEM image shows that layers composed of HfO<sub>2</sub> and Al<sub>2</sub>O<sub>3</sub> have an amorphous structure up to an annealing temperature of 900 °C. The as-grown HfO<sub>2</sub> and Al<sub>2</sub>O<sub>3</sub> film thicknesses are consistent with previously reported MEIS data. The boundary between Al<sub>2</sub>O<sub>3</sub> and HfO<sub>2</sub> in the Al<sub>2</sub>O<sub>3</sub>/HfO<sub>2</sub>/Si stack structure is

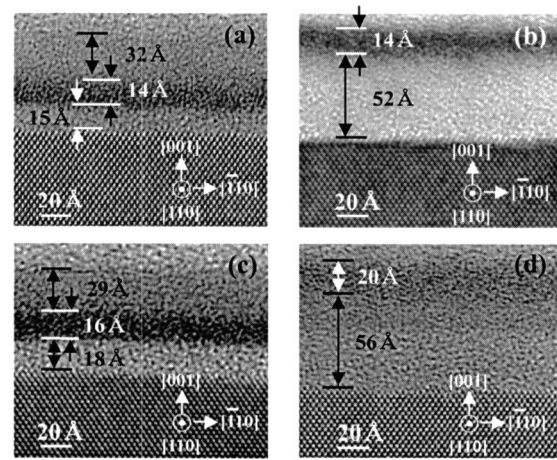


FIG. 2. HRTEM images of (a) an as-grown Al<sub>2</sub>O<sub>3</sub> (30 Å) film with a buffer layer of HfO<sub>2</sub> film (15 Å) on an oxidized Si and (b) an as-grown HfO<sub>2</sub> film (15 Å) with a buffer layer of Al<sub>2</sub>O<sub>3</sub> (30 Å) on an oxidized Si. Images of the films annealed at 900 °C for 5 min in a N<sub>2</sub> ambient: (c) an Al<sub>2</sub>O<sub>3</sub> (30 Å) film with a buffer layer of HfO<sub>2</sub> film (10 Å) on an oxidized Si and (d) a HfO<sub>2</sub> film (10 Å) with a buffer layer of Al<sub>2</sub>O<sub>3</sub> (30 Å) on an oxidized Si.

maintained after the annealing treatment, while that for HfO<sub>2</sub>/Al<sub>2</sub>O<sub>3</sub>/Si is not clear and a gradual change in contrast with the relative quantity of Hf and Al contents can be observed. Moreover, a distinct increase in the film thickness in the HfO<sub>2</sub>/Al<sub>2</sub>O<sub>3</sub>/Si stack structure after the annealing treatment was observed as shown in MEIS data, although the oxidized Si layer on the film surface cannot be clearly discriminated. These results are in good agreement with the MEIS data, which indicates intermixing between Al<sub>2</sub>O<sub>3</sub>/HfO<sub>2</sub> as well as the diffusion of Si (Fig. 3).

Changes in chemical state with stack structure were investigated using XPS. The binding energy of Hf in Hf silicate formation is shifted to a higher position because the more ionic Hf-oxide would be expected to become even more ionic after the formation of the complex oxide, whereas the Si of the more covalent oxide should experience a corresponding covalence under reduced Madelung and relaxation effects.<sup>9</sup> Thus, the peak shift of Hf to higher binding energy in the as-grown Al<sub>2</sub>O<sub>3</sub>/HfO<sub>2</sub>/Si structure indicates that the Hf silicate layer is formed on the contact area between HfO<sub>2</sub>/Si, while the formation of silicate layer is suppressed in the as-grown HfO<sub>2</sub>/Al<sub>2</sub>O<sub>3</sub>/Si structure.<sup>10,11</sup> The high

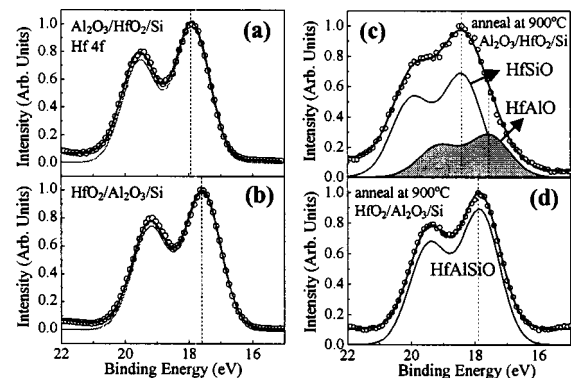


FIG. 3. XPS spectra of annealed films at 900 °C for 5 min in a N<sub>2</sub> ambient: (a) and (b) Hf 4f spectra of as-grown films with stack structures of Al<sub>2</sub>O<sub>3</sub>/HfO<sub>2</sub>/Si and HfO<sub>2</sub>/Al<sub>2</sub>O<sub>3</sub>/Si (30 Å), respectively. (c) and (d) Hf 4f spectra of annealed films at 900 °C with stack structures of Al<sub>2</sub>O<sub>3</sub>/HfO<sub>2</sub>/Si and HfO<sub>2</sub>/Al<sub>2</sub>O<sub>3</sub>/Si (30 Å), respectively.

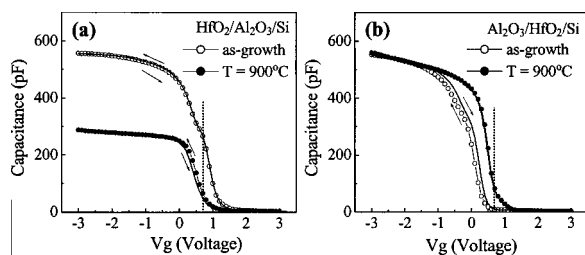


FIG. 4.  $C$ - $V$  curves of (a) a  $\text{HfO}_2(15 \text{ \AA})/\text{Al}_2\text{O}_3(30 \text{ \AA})/\text{Si}$  and (b) an  $\text{Al}_2\text{O}_3(30 \text{ \AA})/\text{HfO}_2(15 \text{ \AA})/\text{Si}$ . The  $C$ - $V$  curves for films annealed at  $900 \text{ }^\circ\text{C}$  for 5 min in a  $\text{N}_2$  ambient are also provided in (a) and (b). The line indicates a zero flatband voltage when a Pt electrode with a workfunction of 5.65 eV is used.

binding energy of  $\sim 18 \text{ eV}$  for the  $\text{Hf } 4f_{7/2}$  of the mixed oxide with  $\text{HfO}_2$ ,  $\text{Al}_2\text{O}_3$ , and  $\text{SiO}_2$ , after the annealing treatment, would be caused by the characteristic differences between ionic and covalent bonding. The broad  $\text{Hf } 4f$  peak in the annealed samples is caused by various chemical states, depending on the degree of intermixing among  $\text{Hf}(\text{Si})\text{O}_x$ ,  $\text{Al}_2\text{O}_3$ , and  $\text{SiO}_x$ . In particular, broadening of  $\text{Hf } 4f$  peak in the annealed  $\text{Al}_2\text{O}_3/\text{HfO}_2/\text{Si}$  structure is increased because of incompletely intermixed layer of  $\text{HfAlO}$  between  $\text{Al}_2\text{O}_3$  and  $\text{Hf}(\text{Si})\text{O}_x$  in the depth direction as shown in the MEIS spectra. On the other hand, completely mixed layer of  $\text{HfAl-SiO}$  is uniformly formed in the annealed  $\text{HfO}_2/\text{Al}_2\text{O}_3/\text{Si}$  structure, resulting from the interdiffusion between  $\text{HfO}_2/\text{Al}_2\text{O}_3$  and the diffusion of Si from Si substrate.

We also investigated changes in the dielectric characteristics by measuring accumulation capacitances. The characteristics of the  $C$ - $V$  curve in the stack structures are shown in Fig. 4. The maximum capacitance value of as-grown films has almost the same value in both structures with different buffer layers. Moreover, in the  $\text{Al}_2\text{O}_3/\text{HfO}_2/\text{Si}$  structure, the accumulation capacitance value is maintained after the annealing treatment, although the thicknesses of the layers with different dielectric constants are changed as shown in TEM and MEIS data. The slight intermixing in the structure after annealing treatment can result in a higher capacitance, assuming the resulting dielectric constant of the mixed oxide lies on intermediate value between the pure oxide values. This increase in capacitance can be offset by the slight increase in interfacial  $\text{SiO}_2$  thickness seen in TEM data. Thus, no change in accumulation capacitance value reflects above two opposite results. It is noteworthy that the change in dielectric constant after the annealing treatment shows a very different tendency, i.e., the accumulation capacitance in the  $\text{HfO}_2/\text{Al}_2\text{O}_3/\text{Si}$  structure is drastically decreased after the annealing treatment, but no change in the  $\text{Al}_2\text{O}_3/\text{HfO}_2/\text{Si}$  structure is detected. The most plausible possibility based on the previous MEIS data is that the decrease of the accumulation capacitance in the  $\text{HfO}_2/\text{Al}_2\text{O}_3/\text{Si}$  structure resulted from the  $\text{SiO}_2$  layer formation on the film surface caused by the diffusion of Si from Si substrate and its oxidation during the annealing process. Therefore, we conclude that the change in stoichiometry in the film as a result of Si incorporation can affect the dielectric constant, resulting in a decrease in accumulation capacitance. The flatband voltage in the as-grown film of  $\text{Al}_2\text{O}_3/\text{HfO}_2/\text{Si}$  structure is shifted to

the negative direction as shown in Fig. 4(b), which indicates that the positive trap charges are contained in the as-grown film. The positive trap charges decrease with increasing annealing temperature. For  $\text{Al}_2\text{O}_3$  in contact with  $\text{SiO}_2$ , the negative charge is located at the interface between the  $\text{Al}_2\text{O}_3$  and  $\text{SiO}_2$ , while for the  $\text{HfO}_2$  film, the positive charge is in the film.<sup>3,8</sup> The two types of trap charges are compensated by each of the other layers, resulting in a reduced flatband voltage shift. Thus, the decrease in positive trap charge in the  $\text{Al}_2\text{O}_3/\text{HfO}_2/\text{Si}$  film after an annealing treatment at  $900 \text{ }^\circ\text{C}$  is caused by the partially intermixed alloy with a negative trap charge structure, which compensates for the positive trap charge in the as-grown film. Moreover, since the quantity of the trap charge is dependent on the depth position and interfacial characteristics, the resulting flatband voltage shift is influenced by the stack structure. In the  $\text{HfO}_2/\text{Al}_2\text{O}_3/\text{Si}$  structure, the shift in the as-grown film is insignificant. However, when the stack structure almost changes into an alloy film after annealing treatment at  $900 \text{ }^\circ\text{C}$ , a flatband voltage is a little shifted to lower direction. Johnson *et al.* reported that  $\text{Hf } d$  states of the alloy act as localized electron traps, which is the opposite shift direction compared to our data.<sup>8</sup> The difference can be explained by the fact that the intermixing of Si, which is observed using MEIS data as shown in Fig. 1(a), significantly affects the total effective charge of the film.

In summary, the thermal stability and the structural characteristics of  $\text{Al}_2\text{O}_3$ - $\text{HfO}_2$  bilayer films are demonstrated in this study. Structural stability is maintained in the  $\text{Al}_2\text{O}_3/\text{HfO}_2/\text{Si}$  structure, but not in the  $\text{HfO}_2/\text{Al}_2\text{O}_3/\text{Si}$  structure. In particular, the diffusion of Si atoms from the Si substrate has a major effect on thermal stability. The diffusion of Si atoms also changes the dielectric constant as well as the oxide trap charge density.

This work was supported by the National Program for Tera-level Nanodevices of the Ministry of Science and Technology as one of the 21 Century Frontier Programs.

<sup>1</sup>I. C. Kizilyalli, R. Y. S. Huang, and P. K. Roy, *IEEE Electron Device Lett.* **19**, 423 (1998).

<sup>2</sup>D. Park, Y.-C. King, Q. Lu, T.-J. King, C. Hu, A. Kalnitsky, S.-P. Tay, and C. C. Cheng, *IEEE Electron Device Lett.* **19**, 441 (1998).

<sup>3</sup>B. H. Lee, L. Kang, R. Nieh, W.-J. Qi, and J. C. Lee, *Appl. Phys. Lett.* **76**, 1926 (2000).

<sup>4</sup>L. Manchanda, W. H. Lee, J. E. Bower, F. H. Baumann, W. L. Brown, C. J. Case, R. C. Keller, Y. O. Kim, E. J. Laskowski, M. D. Morris, R. L. Opila, P. J. Silvermann, T. W. Sorsch, and G. R. Weber, *Tech. Dig. - Int. Electron Devices Meet.* **1998**, 605.

<sup>5</sup>G. Lucovsky and G. B. Rayner, Jr., *Appl. Phys. Lett.* **77**, 2912 (2000).

<sup>6</sup>M.-Y. Ho, H. Gong, G. D. Wilk, B. W. Busch, M. L. Green, W. H. Lin, A. See, S. K. Lahiri, M. E. Loomans, Petri I. Räisänen, and T. Gustafsson, *Appl. Phys. Lett.* **81**, 4218 (2002).

<sup>7</sup>R. S. Johnson, J. G. Hong, C. Hinkle, and G. Lucovsky, *J. Vac. Sci. Technol. B* **20**, 1126 (2002).

<sup>8</sup>L. G. Gosset, J.-F. Damlencourt, O. Renault, D. Rouchon, Ph. Holliger, A. Ermolieff, I. Trimaille, J.-J. Ganem, F. Martin, and M.-N. Séméria, *J. Non-Cryst. Solids* **303**, 17 (2002).

<sup>9</sup>M. J. Guittet, J. P. Crocombette, and M. Gautier-Soyer, *Phys. Rev. B* **63**, 125117 (2001).

<sup>10</sup>M.-H. Cho, D. W. Moon, K. H. Min, R. Sinclair, S. K. Kang, D.-H. Ko, J. H. Lee, J. H. Gu, and N. I. Lee, *Appl. Phys. Lett.* **84**, 571 (2004).

<sup>11</sup>C. Morant, L. Galan, and J. M. Sanz, *Surf. Interface Anal.* **16**, 304 (1990).